ADVANCES IN INORGANIC CHEMISTRY AND RADIOCHEMISTRY, VOL. 26

ONE-DIMENSIONAL INORGANIC PLATINUM-CHAIN ELECTRICAL CONDUCTORS

JACK M. WILLIAMS

Chemistry Division, Argonne National Laboratory, Argonne, Illinois

I. Introduction

The decade of the 1970s has seen an enormous increase in studies of one-dimensional (1-D) electrical conductors, and during that period numerous summary articles and reviews of advances in the field have been published (*1–5*). A 1-D metal may be defined quite simply as one that exhibits metal-like properties in only one direction. For example, four-probe measurements of the electrical conductivity parallel to the Pt chain in 1-D conductors formed from the stacking of square-planar $[Pt(CN)_4]^{2-}$ groups, which comprises the basis of this review, frequently reveal values that are in excess of 10^5 over the conductivity perpendicular to the chain direction. The burgeoning field of studies of 1-D compounds is due to intrinsic scientific interest in unraveling the fundamental chemistry and physics of these unusual materials and, additionally, because of their possible practical uses. There is the likely probability that 1-D materials will find uses in electronic devices and even possibly that a high-temperature superconductor may eventually be discovered.

ISBN 0-12-023626-5

Although 1-D Pt metal chain systems were first synthesized in the mid-1800s (*6, 7*) and described in detail by Levy (*8*) in 1912, it was not until the pioneering work of Krogmann (*9*) in the 1960s that it was fully realized that they were 1-D metals. Numerous reviews of the chemistry and physics (*3–5, 29*) of these intriguing materials were published in the 1970s. A general and up-to-date review of 1-D materials research was published in 1981 (*10*). The most comprehensive review prior to 1975 was that by Miller and Epstein (*5*). The latest and most complete review of the presently known low-dimensional materials has been published as a three-volume treatise (*1*). For this reason it was felt that an up-to-date and state-of-the-art overview, containing selected research highlights pertaining to Pt-chain metals, rather than a detailed tabulation of papers, was most appropriate.

Several classes of 1-D or "low-dimensional" metals are presently known, and they include polymers of the main-group elements [e.g., $(SN)_x$] (*11*), organic polymers such as polyacetylene [$(CH)_x$] (*12*), organic metals [e.g., TTF–TCNQ (*13*)], and superconducting $(TMTSF)_2X$ salts [TMTSF = tetramethyltetraselenafulvalene; X = PF_6^-, SbF_6^-, ClO_4^-, ReO_4^-, and AsF_6^- (*14*)], but they will not be included in this chapter. The main topic of this chapter will be 1-D metals in which the anisotropic metallic properties arise from partial oxidation of a chain of interacting Pt-metal atoms, resulting in very short intrachain metal–metal (M—M) distances (<3.0 Å). The specific focus will be on tetracyanoplatinate complexes formed by overlapping $5d_{z^2}$ orbitals (Fig. 1), because a comprehensive understanding of these partially

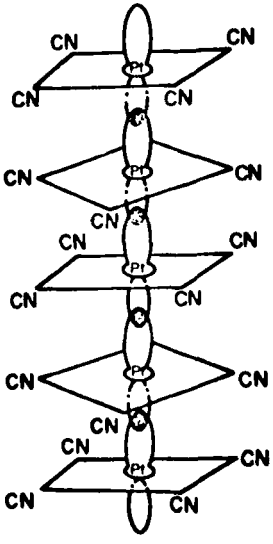

FIG. 1. Illustration of the stacking of square-planar $[Pt(CN)_4]^{X-}$ groups, showing the overlapping of Ptd_{z^2} orbitals.

oxidized (PO) or nonintegral oxidation-state (NIOS) materials has now been achieved (*1*). This chapter will not include such metal-chain systems as $NiPc(I)_x$ (Pc = phthalocyanine; $x \simeq 0.3$–0.4), because M—M distances greater than 3.0 Å are involved, electrical conduction arises primarily from intrachain ligand–ligand interactions, and because a review by Marks and Kalina was published in 1982 (*15*). Chain-forming Ir complexes such as $IrCl(CO)_3$ will not be discussed because a 1982 review of these systems is available (*16*).

The enormous progress that has been made since 1975 in understanding low-dimensional materials has been, in part, due to the in-depth collaborative research between chemists and physicists. Because the fields of chemistry and physics are so inextricably woven with respect to 1-D materials research, it is important that this chapter begin by defining certain terms and concepts related to the basic theories of 1-D conduction.

II. One-Dimensional Band Theory

The first discussion of metallic properties of PO Pt-chain compounds, in terms of a partially filled 1-D band in the chain direction, was given by Krogmann (*9*). In these systems overlap occurs principally between the d_{z^2} and p_z orbitals. The d_{xz}, d_{yz}, and $d_{x^2-y^2}$ orbitals of the metal atom apparently overlap only slightly. When the Pt-atom separations are less than or approximately equal to 3.0 Å, the overlap is substantial and results in the formation of a 1-D band in the chain direction. If the band is partially filled then 1-D metallic properties occur in the metal-atom chain direction. In the case of a system with a d^8 configuration, which must have an even electron count, the partial filling of a band can occur if overlap exists between the filled highest energy band and the empty lowest energy bands (Fig. 2a) or if there is electron removal from the top of the filled highest energy band (Fig. 2b); the latter is the case when partial oxidation of a d^8 ion occurs. A very comprehensive molecular orbital treatment of POTCP metals has been given by Whangbo and Hoffmann (*17*). Although this description (see previous discussion) provides a qualitative introduction to metallic conductivity in one dimension, a more quantitative basis is obtained using the tight-binding band approximation.

The tight-binding band approximation provides a simple theoretical basis for 1-D conduction. In this case we consider a 1-D lattice containing N equally spaced molecules [Fig. 3; see (*18*)] with a repeat distance c. Each isolated molecule has an orbital with energy E_0 that overlaps equivalent orbitals with each of its two surrounding neighbors. From

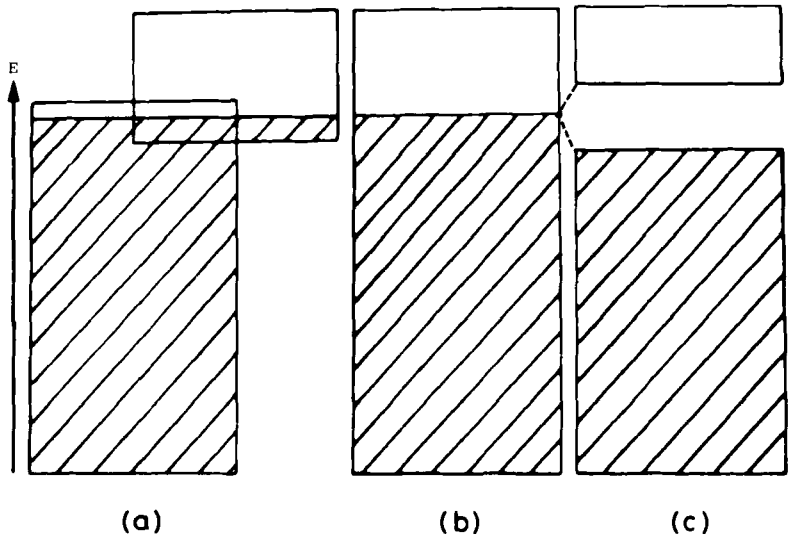

FIG. 2. Illustration of the band structure of a simple 1-D metal. (a) The overlap of full and empty bands. (b) A band that is partially filled. (c) The splitting of a band that is partially filled by a Peierls distortion. [Redrawn from Underhill and Watkins (2).]

tight-binding band theory the orbital energies in the delocalized 1-D array are given by

$$E_i(\mathbf{k}) = E_0 - w\cos(\mathbf{k}c) \equiv E_i(\mathbf{k}),$$

where the allowed values of the wavevector $\mathbf{k}$ and the energies E_i are quantized. As shown in Fig. 3a, the allowed energy levels are very closely spaced above and below that of the isolated molecule E_0, thereby giving the appearance of a continuum. The bandwidth $2W$ forms the boundary of the continuum and comprises N orbitals, which can contain $2N$ electrons. The nearest-neighbor transfer integral t is related to the bandwidth by $2W = 4t$. The density of states per unit energy per spin $D(E)$ (Fig. 3b) is derived from the fact that the wave vector $\mathbf{k}$ has N equally spaced values between $-\pi/c$ and $+\pi/c$.

It is now important to discuss *distortions* in molecular systems and the resulting effects on the total electronic energy of such an ensemble. The familiar Jahn–Teller theorem states that a nonlinear molecular system in a degenerate electronic state is unstable and will be distorted in a manner that will result in lower symmetry and a splitting in the degenerate state. The overall result is a decrease in the total electronic energy of the system.

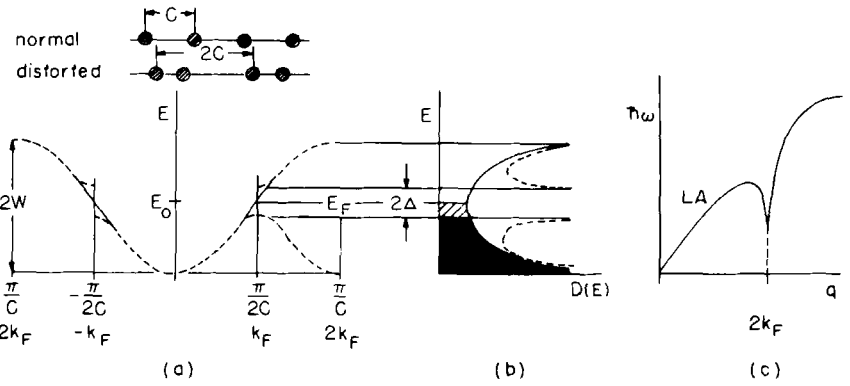

FIG. 3. Anomalies associated with a half-filled conduction band in a 1-D metal. (a) Formation of a band gap at $\mathbf{k}_F$ due to a Peierls distortion of the 1-D lattice. (b) Plot of the density of states per unit energy per spin. (c) A giant Kohn anomaly at $\mathbf{q} = 2\mathbf{k}_F$ in the LA branch of the phonon dispersion. [Adapted from Renker and Comés (*18*).]

In like fashion, Peierls (*19*) and Frohlich (*20*) have shown that a 1-D conductor is also inherently unstable with respect to a lattice distortion. A Peierls transition in an exactly half-filled band (Fig. 3a) causes a lattice distortion in which the molecules dimerize, and this results in the formation of a band gap at the Fermi wave vector $\mathbf{k} = \pi/2c$. It then follows that a Peierls transition in a metal-atom chain converts a 1-D metal into either a semiconductor or an insulator because of the opening of a band gap at the Fermi surface. For a semiconductor the band gap is twice the activation energy for conduction (Δ) and can be determined from electrical-conduction studies performed at variable temperatures. In passing it should be pointed out that the Peierls theory assumes $T = 0$ K, and in reality the band gap becomes temperature dependent at $T \gg 0$ K. At some finite temperature the band gap disappears and an undistorted metallic state exists. In a real 3-D crystalline system the occurrence of metal–insulator transitions occurs at $T \gg 0$ K and is the direct result of coupling between conduction-band electrons and the phonon mode at wave vector $2\mathbf{k}_F$. This in turn produces the *Kohn anomaly* (*21*), which is shown in Fig. 3c. Thus when the energy $\hbar\omega$ of the $2\mathbf{k}_F$ phonon $\equiv 0$, at some finite transition temperature, a static lattice distortion occurs.

It was Frohlich (*20*) who proposed that a distortion in a 1-D metal chain would result in formation of a charge-density wave (CDW) because of the production of a periodic potential by the lattice vibration occurring at $2\mathbf{k}_F$ [Fig. 4; see also (*22*)]. It was further pointed out that if at some point the CDW is not "pinned" in a crystal lattice, these waves

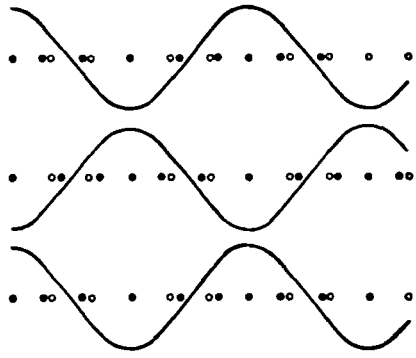

FIG. 4. Three-dimensional ordering caused by an electronic charge-density wave (CDW). For one wave, the relationship of the $2k_F$ lattice distortion and the CDW is shown. ○, Undistorted; ●, distorted lattice sites. [Redrawn from Toombs (*22*).]

produce a moving potential that might result in increased conductivity and, possibly, superconductivity (*20*). A practical consequence of this argument is that when a CDW does become pinned at some finite temperature a metal–insulator type transition occurs. Therefore it is obvious that a 1-D metal will remain metallic when the distortions due to electron–phonon coupling are overcome by the elastic restoring forces of the lattice. Consequently, the stronger the electron–phonon coupling, the higher the transition temperature to a nonconducting state. Thus the suppression of the Peierls transition in 1-D conductors is a practical problem that offers a considerable challenge with respect to the design and synthesis of new materials. We shall elaborate further on these points in Section IV, in which we discuss the physics associated specifically with 1-D Pt-chain metals.

It was not until 1949 that Mott (*23*) introduced the role of Coulombic repulsion between electrons in band theory. Then in 1964 Hubbard (*24*) proposed a model Hamiltonian that included the effective on-site Coulomb repulsion U and the nearest-neighbor transfer integral t. As a consequence, if $t \ll U$ and there is one electron per site, electron localization occurs and Coulomb repulsion is reduced, and the ground state is an antiferromagnetically coupled insulator or Mott–Hubbard insulator. In the case of $t \gg U$, the gain in energy stabilization from delocalization is greater than that due to electron–electron Coulomb repulsion, and the system should become metallic.

As mentioned previously, the search for high-temperature superconducting materials among 1-D systems has prompted a new look at this phenomenon. The BCS (*25*) theory of superconductivity has as its cor-

nerstone a phonon-driven electron-pairing mechanism. The transition temperature for superconductivity T_c can be predicted from the BCS theory by

$$T_c \simeq \frac{\omega_0}{k_B} \exp\left(\frac{-1}{D(\varepsilon_F)V}\right),$$

where k_B is the Boltzmann constant, ω_0 the lattice Debye frequency, $D(\varepsilon_F)$ the density of states at the Fermi surface, and V constitutes the effective electron–electron attraction. Instability will result at some point if V is increased in the hope of raising T_c. The present known maximum for T_c is approximately 25 K in certain metal-alloy systems. To avoid the instability problem, physicist W. A. Little (*26, 27*) proposed that ω_0 be increased instead by using the much higher frequency associated with an electronically polarizable exciton system. In the exciton model a 1-D spine (e.g., a 1-D metal chain) is surrounded by highly polarizable side groups, and electrons moving along the spine could pair up due to electron–exciton–electron interactions. Although very high T_cs are predicted using Little's theory, the problems associated with syntheses of such systems have not yet been surmounted. Still, refinements of Little's theory have resulted in confirmation of the basic principles, and the predictions appear valid (*28*).

Given this background it is now appropriate to consider in detail the chemistry of 1-D Pt-chain systems.

III. The Chemistry of One-Dimensional Partially Oxidized Tetracyanoplatinate (POTCP) Conductors

This chapter encompasses the presently known 1-D complexes formed by the stacking (Fig. 1) of square-planar tetracyanoplatinate (TCP), [$Pt(CN)_4$, (1)] groups. The large majority of 1-D Pt-chain complexes are TCP derivatives, and, to a much lesser extent, the bisoxalatoplatinates. However, because the latter 1-D salts have been extensively reviewed by Underhill *et al.* (*29*), they will not be discussed here.

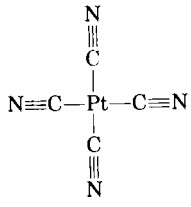

(1)

Complexes containing **1** have a d^8 electron configuration and tend to form square-planar complexes. Krogmann (*9*) and Underhill (*30*) were among the first to point out that the metals given in Table I all have accessible d^8 configurations and, therefore, because of the tendency to form square-planar ligand coordination complexes, could possibly form stacked, columnar structures. Ligands that promote or allow the interactions that favor stacked structures with d_{z^2} orbital overlap are CN^-, CO, Cl^-, and $(C_2O_4)^{2-}$. Although Pt, Ir, and Rh are all known to form 1-D complexes, those of Pt are by far the most predominant.

Although numerous $Pt^{2.0+}$ TCP salts are known to stack in a crystal in such a manner as to form Pt-atom chains, the Pt—Pt distances always exceed 3.0 Å [versus 2.78 Å (*31*) for Pt metal], and the complexes are not metallic. The presently known, and well-characterized, salts of $Pt^{2.0+}$ are given in Table II.

As indicated in Table II, the known TCP complexes of $Pt^{2.0+}$ have a wide range of colors, and their d_{M-M} separations are typically 0.3–0.8 Å longer than in Pt metal. They are nonmetallic in appearance and are electrical insulators because they possess a filled d_{z^2} band {e.g., the conductivity $\sim 5 \times 10^{-7}\ \Omega^{-1}\ cm^{-1}$ for $K_2[Pt(CN)_4] \cdot 3H_2O$}.

A. The Synthesis of One-Dimensional POTCP Metals

In order for metallic properties to arise it is necessary for partial oxidation ($Pt^{2.0} \rightarrow Pt^{2.0+x}$) to occur to form a salt with Pt in a NIOS. Salts of **1**, upon partial oxidation, form POTCP complexes containing $Pt^{2.0+x}$ ($x \cong 0.19$–0.4), which in the crystalline state always have *intra*-chain metal–metal distances (d_{M-M}) of less than 3.0 Å, as opposed to the d_{M-M} spacings given in Table II.

Partial oxidation of a $Pt^{2.0+}$ complex, with the resultant production of a NIOS $Pt^{2.0+x}$ salt with a partially filled band, may be accomplished (*46–49*) by (1) mixing solutions containing the desired $Pt^{2.0+}$ and $Pt^{4.0+}$ salt, (2) chemical oxidation in solution of the appropriate $Pt^{2.0+}$ salt using H_2O_2, or (3) electrolysis of a $Pt^{2.0+}$-containing solution (dc volt-

TABLE I

Metals Having Accessible d^8 Electron Configurations

Configuration	Metal (oxidation state)			
$3d^8$	Fe(0)	Co(+1)	Ni(+2)	Cu(+3)
$4d^8$	Ru(0)	Rh(+1)	Pd(+2)	Ag(+3)
$5d^8$	Os(0)	Ir(+1)	Pt(+2)	Au(+3)

age source and a potential of ~0.75–1.5 V). Method (3) is the preferred procedure at this time because crystal growth on the Pt electrodes is very rapid, namely, seconds or minutes, and well-formed single crystals are easily produced. POTCP complexes may also be grown in this same manner using Au electrodes, and no Au is incorporated in the final product (*50*). In many cases [e.g., $(FHF)^-$ salts (*51*)] method (3) is the only possible route because the appropriate $Pt^{4.0+}$ salt cannot be prepared. When method (1) is used the appropriate tetravalent TCP complex is synthesized by the addition of an excess of oxidant to the $Pt^{2.0+}$ starting material. In the future it may be possible to synthesize POTCP complexes using the $Pt(H_2O)_4^{2+}$ species (*52, 53*). It is important to point out that the success of all of these methods depends on the relative insolubility of the POTCP complex in aqueous solution. In turn, the POTCP salts may be crystallized from aqueous solution un-

TABLE II

THE WELL-CHARACTERIZED SALTS OF TETRACYANOPLATINATE (II)

Compound	Color	Crystal system	d_{Pt-Pt}(Å)[a]	References
$Sr[Pt(CN)_4] \cdot 3H_2O$	Violet	Monoclinic	3.09	(*32*)
$Mg[Pt(CN)_4] \cdot 7H_2O$	Red	Tetragonal	3.155	(*32, 33*)
$Ba[Pt(CN)_4] \cdot 2H_2O$	Dark Red	Orthorhombic	3.16	(*9*)
$Ba[Pt(CN)_4] \cdot 4H_2O$	Yellow-green	Monoclinic	3.321(3)	(*32, 34*)
$Er_2[Pt(CN)_4]_3 \cdot 21H_2O$	—	—	3.17	(*35*)
$Li_2[Pt(CN)_4] \cdot xH_2O$	—	—	3.18	(*36*)
$Dy_2[Pt(CN)_4]_3 \cdot 21H_2O$	—	Orthorhombic	3.18	(*35*)
$Tb_2[Pt(CN)_4]_3 \cdot 21H_2O$	—	—	3.18	(*35*)
$Y_2[Pt(CN)_4]_3 \cdot 21H_2O$	—	Orthorhombic	3.18	(*35*)
$KLi[Pt(CN)_4] \cdot 2H_2O$	—	—	3.20	(*37*)
$K_2Sr[Pt(CN)_4] \cdot 2H_2O$	Violet-red	Monoclinic	3.21	(*36*)
$KNa[Pt(CN)_4] \cdot 3H_2O$	—	Monoclinic	3.26(2)	(*38, 39*)
$(NH_4)_2[Pt(CN)_4] \cdot 2H_2O$	—	—	3.26	(*36*)
$K_2Sr[Pt(CN)_4] \cdot 6H_2O$	Yellow-green	Monoclinic	3.33	(*32*)
$Sm_2[Pt(CN)_4]_3 \cdot 18H_2O$	—	—	3.35	(*40*)
$Mg[Pt(CN)_4] \cdot 4.5H_2O$	Yellow	Triclinic	3.36	(*32*)
$Eu_2[Pt(CN)_4]_3 \cdot 18H_2O$	—	—	3.37	(*40*)
$Ca[Pt(CN)_4] \cdot 5H_2O$	Yellow	Orthorhombic	3.38	(*32*)
$Rb_2[Pt(CN)_4] \cdot 1.5H_2O$	Green	Monoclinic	3.421(2)	(*41*)
$K_2[Pt(CN)_4] \cdot 3H_2O$	—	Orthorhombic	3.478(1)	(*36, 42*)
$Cs_2[Pt(CN)_4] \cdot H_2O$	—	Hexagonal	3.545(1)	(*43, 44*)
$Sr[Pt(CN)_4] \cdot 5H_2O$	Colorless	Monoclinic	3.60	(*32*)
$Na_2[Pt(CN)_4] \cdot 3H_2O$	Colorless	Triclinic	3.71	(*45*)[b]

[a] Values in parentheses are estimated standard deviations of the distance given.

[b] Four independent spacings exist in this salt (3.65, 3.69, 3.75, and 3.75 Å).

der the appropriate conditions. A large number of POTCP complexes and their starting materials have been prepared (see Table III) and the syntheses independently checked (*46–49*).

B. Anion-Deficient and Cation-Deficient Complexes

We now turn to a discussion of the properties of the known POTCP complexes. A summary of the physical property data for all well-characterized POTCP complexes is given in Table III. From this tabulation it is apparent that a wide range of POTCP complexes have been well characterized. As shown in Table III there exist two basic types of POTCP complex as follows.

1. *Anion-Deficient (AD) Complexes.* In AD complexes PO of the Pt atom and partial filling of the d_{z^2} band are achieved by the formation of a compound that contains a nonstoichiometric number of anions (X). The general formula for these materials is $M_i[Pt(CN)_4]X_n \cdot jH_2O$ [where M is a monovalent cation, i an integer (1–3), n nonintegral and <1.0, and j has values of 0–3]. The molecular structures of AD salts vary significantly, as do the electrical properties, between the hydrated and anhydrous AD derivatives (see following discussion).

2. *Cation-Deficient (CD) Complexes.* In CD materials the nonstoichiometry occurs when the cation content is nonintegral. The general formula for these materials is $M_i[Pt(CN)_4] \cdot jH_2O$ [where i is nonintegral ($1 < i < 2$) and j always appears to be > 1].

The structural and electronic properties of 1-D POTCP metals are highly dependent on the nature of the species that constitute the crystal lattice. Before discussing the basic structural features of POTCP complexes it will be helpful if we first discuss the concept of the degree of partial oxidation (DPO) in these materials.

The Degree of Partial Oxidation of Pt in POTCP Complexes

A knowledge of the DPO of the metal atom in POTCP salts is critically important to the understanding of the associated solid-state properties. The DPO can be determined as follows.

1. By iodimetric titration of the POTCP complex in solution, the $Pt^{2.0}:Pt^{4.0}$ ratio may be determined.

2. By chemical analysis, the cation : anion mole ratio may be determined. This method is not without difficulty because in certain cases, for example, $(NH_4)_2(H_3O)_{0.17}[Pt(CN)_4]Cl_{0.42} \cdot 2.83H_2O$ [ACP(Cl)], the method yielded (before it was surmised that the complex contained

H_3O^+ due to crystallization from acid solution) DPO = 0.42, which was far too high for $d_{M-M} \simeq 2.92$ Å (*61, 62*). By comparison, the DPO (see Table III) for KCP(Br) is 0.3, and the d_{M-M}, which should be greater than that in ACP(Cl), is actually less (2.87 Å). This problem was clarified using method (3).

3. By the use of X-ray diffuse-scattering (XDS) techniques, the DPO may be determined. This method appears to be the most accurate for POTCP materials and can be used to understand the known "modulations" of the average structure, as determined by X-ray or neutron crystallography. For an introduction to the uses of XDS techniques, see Section III,D and (*77–79*).

Before discussing XDS "structural" studies of POTCP metals, we must first understand their basic structural types.

C. The Crystal and Molecular Structures of POTCP Metals

In order for us to understand the physical properties associated with POTCP materials, it is important that we begin with a description of some of their basic structural features and the variations produced when different cations and anions are introduced.

Given that a POTCP complex will always contain stacked $Pt(CN)_4^{2.0+x}$ groups, the basic molecular geometries that can be formed now appear somewhat predictable (*3*). There is obviously a certain "basic integrity" to the metal-atom chain in a POTCP salt, because the chain itself behaves in an *accordion*-like fashion upon partial oxidation, that is, the Pt—Pt distances vary over only a small range of approximately 0.2 Å for these materials (see Table III). The Pt—Pt distances and the DPO of the metal atom are now known to behave in a predictable manner (*80*). In general, as the DPO increases and the d_{M-M} decreases the conductivity of a POTCP salt increases.

1. Anion-Deficient POTCP Salts

a. Hydrated Derivatives. Krogmann and Hausen (*81*) were the first to report the crystal structure of the prototypical AD salt $K_2[Pt(CN)_4]Br_{0.3} \cdot 3H_2O$ ("KCP(Br)" or "KCP"). The structural description was slightly in error due to an incorrect distribution of the molecular contents of the unit cell, as pointed out from a neutron-diffraction study by Williams *et al.* (*82*), but the most important feature, the Pt-atom chain, was elucidated, thereby providing a structure of pivotal importance.

TABLE III

PARTIALLY OXIDIZED TETRACYANOPLATINATE METALS: CRYSTAL STRUCTURE AND CONDUCTIVITY DATA

Complex	Abbreviation	Space group[a]	Intrachain separation[b] d_{Pt-Pt} (Å) (T = 298K)	Conductivity[c] (ohm^{-1} cm^{-1})	Color
Pt metal			2.775[d]	9.4×10^4	Metallic
$K_2[Pt(CN)_4]Br_{0.30} \cdot 3H_2O$	KCP(Br)	$P4mm$[a,e]	2.89	4–1050	Bronze[f]
$K_2[Pt(CN)_4]Cl_{0.30} \cdot 3H_2O$	KCP(Cl)	$P4mm$[g]	2.87	~200	Bronze[f]
$K_2[Pt(CN)_4]Br_{0.15}Cl_{0.15} \cdot 3H_2O$	KCP(Br, Cl)	$P4mm$[h]	—	—	—
$Rb_2[Pt(CN)_4]Cl_{0.3} \cdot 3H_2O$	RbCP(Cl)	$P4mm$[i,j]	2.877(8) and 2.924(8) at T = 298K[i]; 2.885(6) and 2.862(6) at T = 110K[j]	10[k]	Bronze
$Cs_2[Pt(CN)_4]Cl_{0.3}$	CsCP(Cl)	$I4/mcm$[l]	2.859(2)	~200[m]	Bronze
$(NH_4)_2(H_3O)_{0.17}[Pt(CN)_4]Cl_{0.42} \cdot 2.83H_2O$	ACP(Cl)	$P4mm$[n]	2.910(5) and 2.930(5)	0.4[o]	Bronze
$Cs_2[Pt(CN)_4](N_3)_{0.25} \cdot 0.5H_2O$	CsCP(N_3)	$P\bar{4}b2$[p]	2.877(1)	40–270[q]	Reddish–copper
$Rb_3(H_3O_{0.x}[Pt(CN)_4]9O_3SO \cdot H \cdot OSO_3)_{0.49} \cdot (1 - x)H_2O$	RbCP(DSH)	$P\bar{1}$[r]	2.826(1)	[s]	Copper
$K_{1.75}[Pt(CN)_4] \cdot 1.5H_2O$	K(def)TCP	$P\bar{1}$[t]	2.965(1) and 2.961(1)	115–125[u,v]	Bronze

$Rb_{1.75}[Pt(CN)_4] \cdot xH_2O$	Rb(def)TCP	V^{u}	2.94[x]	1[v]	Bronze
$Cs_{1.75}[Pt(CN)_4] \cdot xH_2O$	Cs(def)TCP	V^{w}	2.88	~25[y]	Bronze
$K_2[Pt(CN)_4](FHF)_{0.30} \cdot 3H_2O$	$KCP(FHF)_{0.3}$	$P4mm^{z}$	2.918(1) and 2.928(1)	[s]	Reddish–bronze[aa]
$Rb_2[Pt(CN)_4](FHF)_{0.40}$	$RbCP(FHF)_{0.4}$	$I4/mcm^{bb}$	2.798(1)	1600[cc] 2300[dd]	Gold
$Rb_2[Pt(CN)_4](FHF)_{0.26} \cdot 1.7H_2O$	$RbCP(FHF)_{0.26}$	$C2/c^{w}$	2.89	[s]	Greenish–bronze[aa]
$Cs_2[Pt(CN)_4](FHF)_{0.39}$	$CsCP(FHF)_{0.4}$	$I4/mcm^{ee}$	2.833(1)	2000[cc] 1600[dd]	Reddish–gold[aa]
$Cs_2[Pt(CN)_4](FHF)_{0.23}$	$CsCP(FHF)_{0.23}$	$I4/mcm^{w}$	2.872(2)	250–350[w]	Reddish–bronze[aa]
$Cs_2[Pt(CN)_4]F_{0.19}$	CsCP(F)	$Immm^{w}$	2.866(1)	[s]	Reddish–gold[aa]
$[C(NH_2)_3]_2[Pt(CN)_4](FHF)_{0.26} \cdot xH_2O$	$GCP(FHF)_{0.26}$	[s]	2.90[ff]	[s]	Bronze
$[C(NH_2)_3]_2[Pt(CN)_4]Br_{0.25} \cdot H_2O$[gg]	GCP(Br)	$I4cm^{gg}$	2.908(2)	11[gg]	Bronze

[a] In space group $P4mm$ the Pt—Pt intrachain distances are not required to be equal, but they often appear so. When they have been determined to be different both distances are given.

[b] Values in parentheses are estimated standard deviations of the distances given.

[c] The range of literature values reported for room temperature four proble DC conductivities are given.

[d] (*31*). [e] (*3*). [f] (*5*). [g] (*54*). [h] (*55*). [i] (*56*). [j] (*57*). [k] (*58*). [l] (*59*). [m] (*60*). [n] (*61*). [o] (*62*). [p] (*63*). [q] (*64*). [r] (*3*), pp. 361–362. [s] (*107*). [t] (*65–67*). [u] (*68*). [v] (*69*).

[v'] The crystal class is monoclinic, but the space group is unknown. The lattice constants for the Cs salt[w] are a = 18.35(1) Å, b = 5.760(3) Å, c = 19.92(1) Å, β = 109.03(4)°; for the Rb salt[u] the lattice constants are a = 10.56(1) Å, b = 33.2(1) Å, c = 11.74(1) Å, β = 114.23(3)°.

[w] J. M. Williams, work in progress.

[x] (*70*). [y] (*71*). [z] (*72*). [aa] (*51*). [bb] (*73*). [cc] (*3*). [dd] (*74*). [ee] (*75*). [ff] (*3*), p. 357. [gg] (*76*).

In KCP(Br) and its isostructural "type-P" [P = primitive (*3*)] derivatives (see Table III, space group $P4mm$), DPO = 0.3, indicating that in the process of oxidation 0.3 electrons per Pt atom have been removed from the highest filled ($5d_{z^2}$) band. Therefore, 1.7 electrons per Pt atom remain in the band, and in the crystal (see Fig. 5) the $[Pt(CN)_4]^{1.7-}$ moieties stack to form linear, metal-atom chains that have *equal intra*atomic Pt—Pt spacings (d_{M-M} = 2.89 Å). The K^+ ions are situated in one-half of the unit cell, and the H_2O molecules, which are located in the other half, form a network of hydrogen bonds between the CN^- ligands and either the Br^- anion at the unit-cell center or the CN^- ligand from a TCP group on an adjacent chain. Adjacent TCP chains are separated by 9.89 Å, which accounts in part for the great anisotropy in the physical properties for KCP derivatives. Therefore, type-P salts are those in which the cations and water molecules do *not* occupy the same molecular plane as the $Pt(CN)_4$ groups. Isostructural halide (Br^-, Cl^-) derivatives of KCP are all nonstoichiometric, and the central portion of the unit cell is alternatively occupied by either a Br^- ion (at ½, ½, ½, labeled Br* in Fig. 5, 60% occupancy) or an H_2O molecule (at

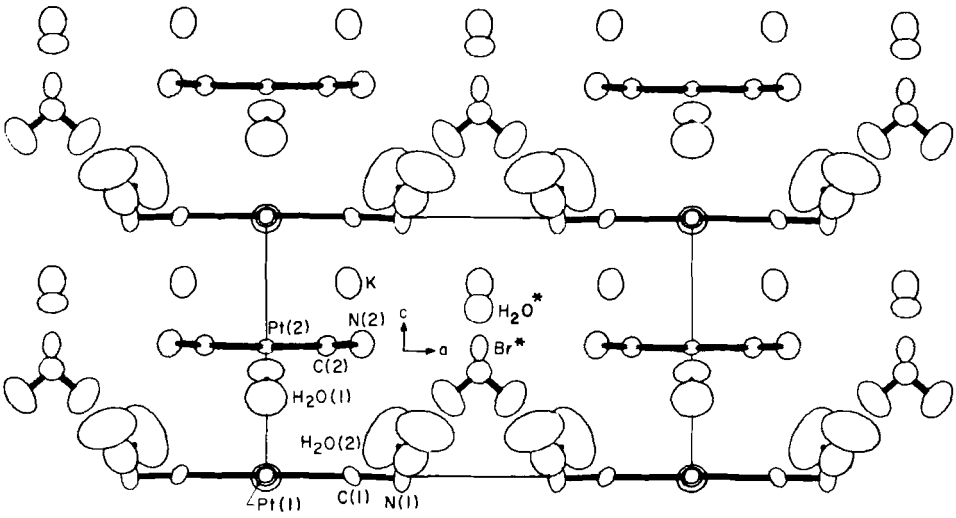

FIG. 5. Structure of the prototypical type-P complex $K_2[Pt(CN)_4]Br_{0.3} \cdot 3H_2O$ [KCP(Br)], shown as a *b*-axis half-cell projection. In type-P 1-D metals (*3*) the cations are interleaved *between* the $Pt(CN)_4$ groups. The independent atoms in the asymmetric unit are identified. The disordered Br^- and H_2O sites are labeled as Br* and H_2O*. The K^+ ions occupy one-half of the unit cell, and the H_2O molecules occupy the other half. Note that the Pt—Pt distances are all equal at 2.89 Å.

½, ½, 0.67, H_2O* in Fig. 5, 40% occupancy). Accompanying the very short intrachain Pt—Pt separation of 2.89 Å is an intrachain torsion angle of 45° between adjacent $[Pt(CN)_4]^{1.7-}$ groups, which apparently minimizes ligand stearic hindrance. Numerous structural studies of KCP(Br, Cl) have been reported (*54, 82, 83*), and the structural architecture of these prototypical salts is well understood.

A discussion of structure–property relationships in KCP analogs would be incomplete if it were not mentioned that these compounds undergo gradual transitions from an ambient-temperature conducting state [σ = 5–800 Ω^{-1} cm^{-1} (*84*)] to a low-temperature insulating state.

From variable-temperature Mössbauer and ESCA studies the electronic equivalence of the Pt atoms in KCP(Br) has been confirmed (*5*). In addition, classical crystallographic studies (*54, 82, 83*) have shown that the structure of KCP(Br) remains basically unchanged, even to liquid-He temperatures. The observation of a giant Kohn anomaly (*77, 85*) and a low-temperature 3-D superlattice (*77–79*) from various XDS and inelastic neutron-scattering studies provides ample evidence for a Peierls distortion and CDW formation in these materials. Therefore, in KCP(Br) the *average* crystallographic structure is invariant with temperature but is "modulated" by a CDW, and the room-temperature response of the $Pt(CN)_4$ groups is that a dynamic, sinusoidal displacement of each Pt atom along each chain occurs with no coherence between neighboring chains. The repeat period of 6.67 c', where c' is twice the d_{Pt-Pt} distance, is exactly that expected for a Peierls distortion. At 77 K and below, a 3-D ordering occurs, and the distortion becomes static. From neutron-scattering studies Lynn *et al.* (*86*) have shown that the sinusoidal Pt-chain distortion, due to the formation of a CDW by the d_{z^2} electrons, involves each atom of the $Pt(CN)_4^{1.7-}$ moiety that "rides" on the CDW. At liquid-He temperature the Pt atom displacement, due to the CDW, is only 0.025 Å from the perfectly equal spacing derived in a classical structure analysis (*86*). Therefore, the average crystallographic structure of KCP(Br) is constant but is modulated by a CDW, to which each $Pt(CN)_4^{1.7-}$ group responds.

Although $Rb_2[Pt(CN)_4]Cl_{0.3} \cdot 3H_2O$ [RbCP(Cl)] has been characterized by single-crystal neutron scattering and XDS (*56*) and appears to be isostructural with KCP(Br), only one halide site per unit cell has been identified. Another significant structural feature is that, although not required by the space-group symmetry, all intrachain Pt—Pt separations in KCP are equal. However, in RbCP(Cl) there is a definite *dimerization* of the linear Pt-atom chain (see Fig. 6). Compared to KCP(Br), it appears that the replacement of the K^+ ion by the larger Rb^+ ion results in lattice expansion along c, which in turn pro-

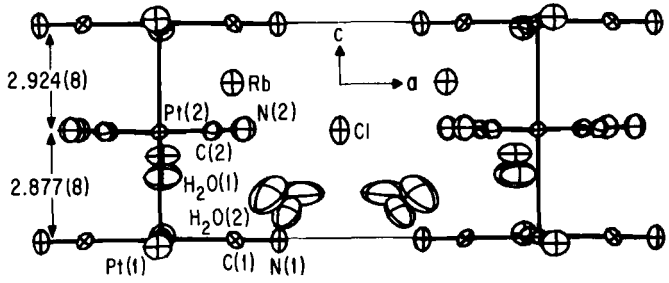

FIG. 6. Structure of $Rb_2[Pt(CN)_4]Cl_{0.3} \cdot 3.0H_2O$ at 298 K, showing the *unequal* Pt—Pt separations in the linear metal-atom chain. The average Pt—Pt distance in the dimerized chain is approximately 0.03 Å longer than in KCP(Br) (Fig. 5). Only one Cl^- site was identified (*56*).

duces larger Pt—Pt spacings in RbCP(Cl). It is therefore reasonable to expect that the electrical conductivity of RbCP(Cl) might be less than that of KCP(Br) due to the longer, dimerized Pt chain.

However, the question of how the electrical conductivity varies with structural changes and temperature in hydrated type-P POTCP salts affords surprising results, as explained here for RbCP(Cl). A low-temperature neutron-diffraction study (*57*) of this salt showed that the degree of dimerization *decreases* with temperature (see Fig. 7) which was unexpected because variable-temperature conductivity studies (*58*) established that the electrical conductivity along the Pt-atom chain also decreases with decreasing temperature in the sequence ACP(Cl) < RbCP(Cl) ≃ KCP(Br) (Fig. 8). Just the opposite results are expected, that is, that as chain dimerization and the associated electron localization decrease, the conductivity should rise. The explana-

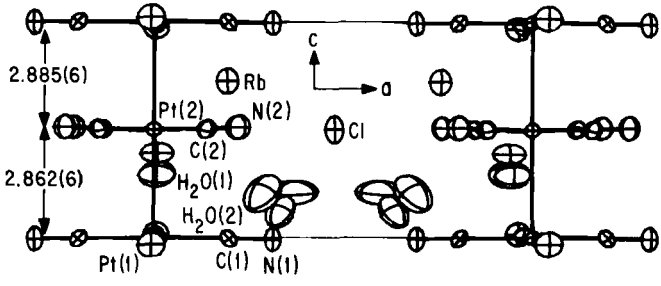

FIG. 7. Unit cell of $Rb_2[Pt(CN)_4]Cl_{0.3} \cdot 3H_2O$, derived from neutron-diffraction data collected at 110 K. Note that the degree of chain dimerization *decreases*, compared to the room-temperature structure (Fig. 6) and that the average Pt—Pt spacing decreases by approximately 0.02 Å at 110 K (see *57*).

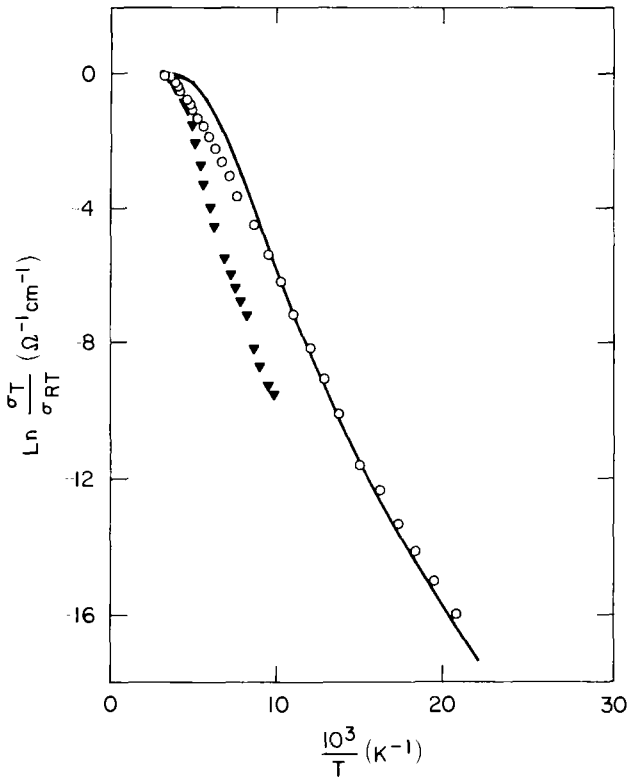

FIG. 8. Temperature dependence of the dc electrical conductivity along the Pt—Pt chain for three type-P isostructural compounds (space group *P4mm*): —, KCP(Br); ○, RbCP(Cl); ▼, ACP(Cl) (see *58*).

tion for this behavior does not lie in the degree of chain dimerization but rather in terms of *differing temperatures* at which there is coupling of the 1-D lattice distortions, or Peierls distortions, which in turn cause the Pt-atom chains to undergo a 3-D ordering transition at a temperature termed T_{3D} (*87*). It appears that there is always a decrease in conductivity in POTCP salts at T_{3D}. The means whereby T_{3D} may be derived and the T_{3D}s for POTCP materials are discussed in Section IV.

It is apparent that although KCP(Br) never undergoes chain dimerization at any temperature, some type-P salts exhibit this behavior, even if the d_{Pt-Pt} is almost that of KCP(Br). A summary of the structural results derived from numerous diffraction studies, in which monovalent cations of differing radius (r^+) have been substituted for K^+, is as follows (*59*).

1. For a given d_{Pt-Pt}, as r^+ increases the probability of dimerization increases.
2. For a given r^+, as d_{Pt-Pt} decreases the probability that dimerization will occur decreases.
3. For a given r^+ the d_{Pt-Pt} tends to depend on the DPO, and therefore the degree of chain dimerization may depend on the DPO.

b. Anhydrous Derivatives. Extensive synthetic studies of POTCP metals at Argonne National Laboratory in the late 1970s resulted in the discovery of a new class of salts, "type-I" (I = body-centered lattice), with markedly different structure–property relationships compared to the hydrated KCP-type derivatives. The most salient structural difference between the hydrated type-P and anhydrous type-I salts is that in the latter the M^+ cations occupy the same molecular plane as the square-planar $Pt(CN)_4$ groups, which maximizes M^+—$^-N{\equiv}C$ interactions. Examples of this class of material are $Cs_2[Pt(CN)_4]Cl_{0.3}$ [(*59*); see Fig. 9], $Cs[Pt(CN)_4](FHF)_{0.38}$ (*75*), $Cs[Pt(CN)_4](FHF)_{0.23}$ (*51*), $Rb_2[Pt(CN)_4](FHF)_{0.4}$ [(*73*); Fig. 10], and pseudo-body-centered $Cs_2[Pt(CN)_4](N_3)_{0.25} \cdot xH_2O$ (*63*). It appears that although the $(FHF)^-$ salts are strictly anhydrous, both $Cs_2[Pt(CN)_4]Cl_{0.3}$ and $Cs_2[Pt(CN)_4](N_3)_{0.25} \cdot xH_2O$ may be slightly hydrated. $Rb_2[Pt(CN)_4](FHF)_{0.4}$ is unique in that it contains the *shortest* Pt—Pt spacing (2.798 Å) and *highest* room-temperature electrical conductivity of any known POTCP salt (*73, 74*). However, all of these derivatives possess type-I molecular architecture, which markedly affects (improves!) the conduction behavior (see following discussion).

The results of variable-temperature electrical-conduction studies of a number of type-I salts have been reported (*60, 74*), and they are

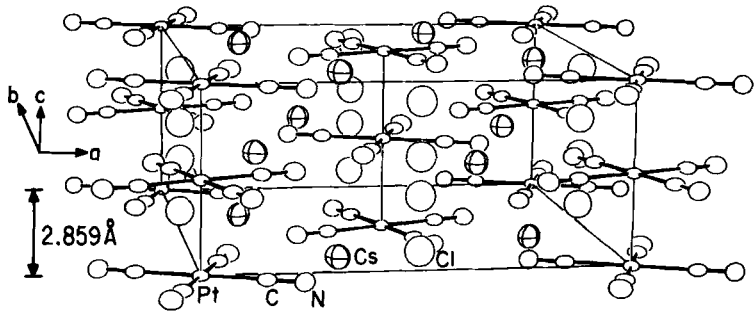

FIG. 9. Unit cell of the type-I 1-D metal, anhydrous $Cs_2[Pt(CN)_4]Cl_{0.3}$, [CsCP(Cl)]. Note that in type-I complexes the cation Cs^+ occupies the same molecular plane as the $Pt(CN)_4$ groups (see *59*).

compared with KCP(Br) in Fig. 11. Metallic conduction is exhibited by KCP(Br) at room temperature, but at low temperature it becomes semiconducting in nature. From Fig. 11 it is apparent that the conduction behavior of $Cs_2[Pt(CN)_4]Cl_{0.3}$ is intermediate between that of KCP(Br) and $Rb_2[Pt(CN)_4](FHF)_{0.4}$.

In all of the known POTCP salts it appears that the room-temperature conductivity $\sigma_\parallel$ is dominated by the *intra*chain Pt—Pt separation, but considerable differences in behavior arise at reduced temperature, depending on the structure type, nature of the cations and anions present, etc. *Inter*chain Pt—Pt distances vary somewhat, and it is noteworthy that in the type-I derivatives enhanced conductivity parallels reduced interchain spacings, {cf. 9.32 Å in $Cs_2[Pt(CN)_4]Cl_{0.3}$, 9.23 Å in $Cs_2[Pt(CN)_4](FHF)_{0.39}$, and 8.97 Å in $Rb_2[Pt(CN)_4](FHF)_{0.4}$}. However, this trend in reduced interchain separation also parallels a reduced intrachain Pt—Pt distance.

From Fig. 11 it is obvious that the decrease in conductivity in passing from room temperature to the lower-temperature semiconducting region is much less for the anhydrous type-I salts compared to the type-P salts. The activation energies in the semiconducting region are approximately 0.02 eV for the bifluoride salts with DPO $\cong$ 0.40 compared to approximately 0.07 eV for KCP(Br), for which DPO = 0.30 (*60*). As discussed in Section IV, the 3-D ordering temperature T_{3D} is a measure of Coulombic interchain coupling and depends to some degree on the presence of hydrogen bonding between $Pt(CN)_4$ groups. Therefore, it is not unexpected that T_{3D} is lowest for type-I salts, as will be shown later (see Fig. 15).

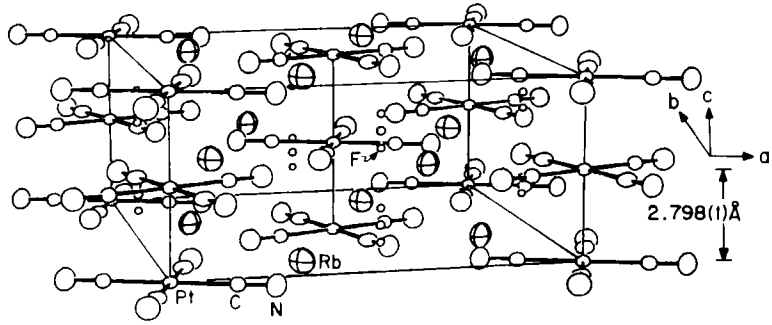

FIG. 10. Perspective view of the unit cell of type-I $Rb_2[Pt(CN)_4](FHF)_{0.4}$ [RbCP(FHF)$_{0.4}$]. The small circles are the partially filled F-atom positions. The Pt—Pt spacing is the *shortest* known for any POTCP 1-D metal (*73*). The corresponding Pt-chain conductivity is the *highest* (~2000 Ω^{-1} cm^{-1} at 298 K) for any known POTCP complex (see *60, 73*).

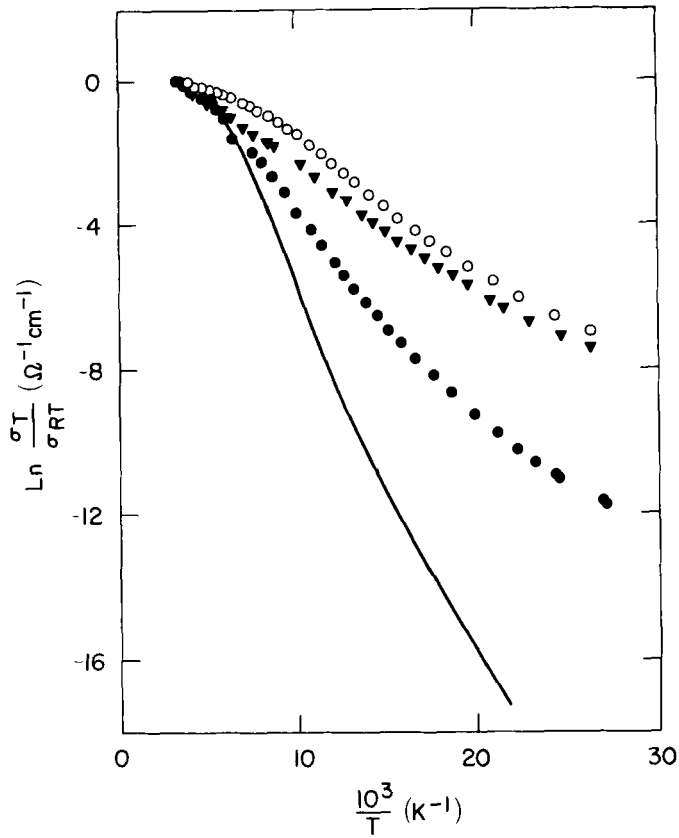

FIG. 11. Temperature dependence of the in-chain dc conductivity for three isostructural type-I compounds (space group *I4/mcm*): ○, $RbCP(FHF)_{0.4}$; ▼, $CsCP(FHF)_{0.4}$; ●, $CsCP(Cl)_{0.3}$ (see *60, 74*). The curve (—) is for type-P KCP(Br) and is shown for comparison purposes.

2. *Cation-Deficient POTCP Salts*

The CD complexes of POTCP metals are few in number compared to the AD derivatives, and only $K_{1.75}[Pt(CN)_4] \cdot 1.5H_2O$ [K(def)TCP, where K(def) = K deficient] has been well characterized (DPO = 0.25) by a variety of physical and theoretical studies [see (*65–67, 88*) and Table III]. A high-precision neutron-diffraction study (*66*) was used to locate all atoms in the structure, including hydrogen, and the derived crystal structure is shown in Fig. 12. The most unusual finding was that K(def)TCP contains the longest Pt—Pt separations (2.96 and 2.97 Å) and the only known bent atom chain in a POTCP salt. From these

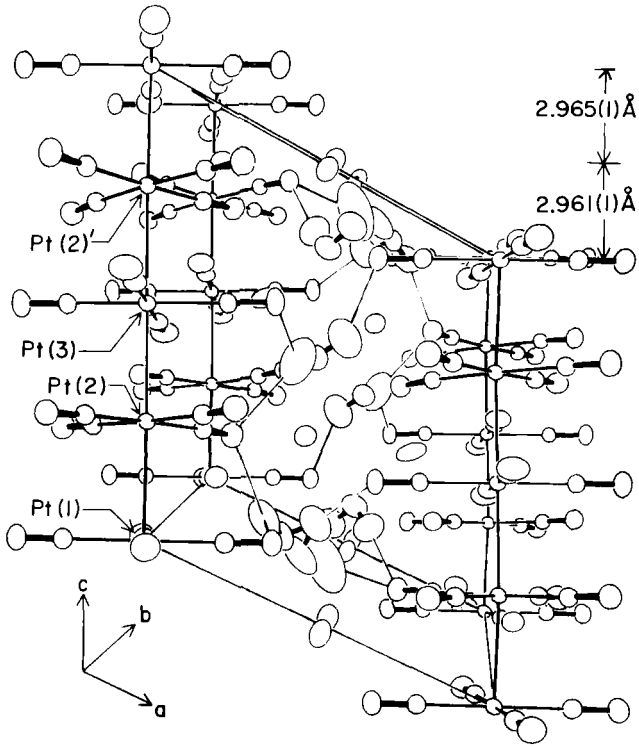

FIG. 12. Unit cell of triclinic $K_{1.75}[Pt(CN)_4] \cdot 1.5H_2O$ [Kdef(TCP)], derived from neutron-diffraction data showing the *non*linear Pt-atom chain [Pt(1)-Pt(2)-Pt(3) = 173.3°], which extends along *c*. Note that the Pt—Pt spacings, which are equal although not required by the space-group symmetry, are the longest for any known POTCP complex (see *65*, *66*).

results it appears that $d_{Pt-Pt} \simeq 3.0$ Å is the upper limit of the *intra*-chain Pt—Pt separation for POTCP formation. Another noteworthy finding was that, even though not required crystallographically as is also the case for KCP, the Pt—Pt separations are essentially equal. XDS studies (*70*) of K(def)TCP have been used to show that it possesses a superlattice structure that is *commensurate* with the Pt-atom chain (*c* axis of the crystal) with a repeat distance $8c'$ (c' = average d_{Pt-Pt}). In KCP derivatives in which DPO = 0.30, XDS studies reveal a superlattice that is *incommensurate* (6.67 c'). The wave vector derived from the XDS studies agrees very well with $2\mathbf{k}_F$ predicted from the chemical stoichiometry (*89*). This may be demonstrated as follows. A completely filled d_{z^2} band would contain a contribution of two electrons from each Pt atom, and the calculated Fermi wave vector would then

be $\mathbf{k}_F = (1.75/2)\pi/c'$. From the XDS study the derived wave vector $\mathbf{k} = 2\pi/8.1\ c'$ or $2\pi(1 - 1/8.1)/c'$, which is in essential agreement with that just predicted. In passing it should be noted that the *nature* (commensurate versus incommensurate) of the superlattice observed in POTCP metals may be an underlying factor in the conductivity trend K(def)TCP $\ll$ KCP(Br).

Three M(def)TCP salts (M = K^+, Rb^+, and Cs^+) have all been shown to be 1-D metals from optical-reflectance studies (*90*). Neutron-scattering studies (*88*) have shown the presence of a Kohn anomaly in K(def)TCP.

Although two independent electrical-conduction studies (*68, 69*) have established that the room-temperature values ($\sigma_\parallel \simeq 100\ \Omega^{-1}\ cm^{-1}$) are the same and also that the conduction *behavior* of K(def)TCP and KCP(Br) is different, the detailed interpretation of the data and the derived zero-temperature band gaps (Δ) and T_{3D}s, respectively, are at some variance. These results and the interpretation derived from an independent Raman scattering study (*91*) have been discussed in detail elsewhere (*92*).

Perhaps the most important finding from all of these studies is that the M(def)TCP salts have physical properties that are considerably different from those of KCP-type analogs, and each of these two sets appears to constitute a separate class. The source of the physical property differences is in part due to the finding that in POTCP materials the observed Peierls distortions are related to the DPO. In fact, an understanding of the relationships between the DPO and the physical parameters used to describe POTCP metals provides the basic information needed for unraveling the physics of these materials.

D. X-Ray Diffuse Scattering and Structural Modulation in POTCP Metals

A characteristic of all 1-D POTCP metals is the existence of a modulated structure (*89*). In the case of a TCP stack (see Fig. 1), this subtle structural feature is best described as a modulation of the *average* atomic positions, which arises from electron–phonon coupling, and it can provide basic information regarding the conduction-band properties of a material.

The prototypical POTCP complex $K_2[Pt(CN)_4]Br_{0.3} \cdot 3H_2O$ ["KCP(Br)" or "KCP"] exhibits both neutron and XDS, which led Comés and co-workers (*77*) to elucidate in detail this phenomenon in KCP(Br). The important concepts for a hypothetical case are illustrated in Fig. 13, in which we assume a 1-D lattice with a one-eighth

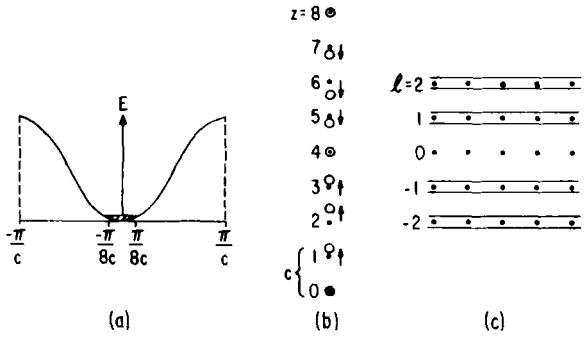

FIG. 13. (a) One-eighth filled band. (b) Sinusoidal lattice distortion with shifts of $\delta = \Delta\sin(2\pi z/8)$ and a period of 8c. (c) X-Ray diffuse-scattering diagram showing diffuse satellite planes around Bragg spots in reciprocal space.

filled band [the actual case for K(def)TCP, with DPO = 0.25]. The band gap is formed at $\mathbf{k}_F = \pi/8c$, which produces a lattice modulation of periodicity 8c. This results in sinusoidal distortions, namely, a CDW (see Fig. 4) along the metal chain. At high temperatures there is no phase correlation between the CDWs of parallel chains in a crystal, and this property may be observed using elastic XDS or neutron diffuse scattering as satellite planes of diffuse scattering in reciprocal space with wave vectors of $2\mathbf{k}_F$. When using X rays and a photographic film, the manifestation of the Peierls distortion (i.e., a CDW) is the presence of weak planes or lines (diffuse lines) about the layer line spots, which are due to normal Bragg scattering (*70*). For POTCP complexes the DPO can be calculated from the position of the diffuse scattering lines using the relationship

$$\text{DPO} = 2(1 - \mathbf{k}_F d_{\text{Pt}-\text{Pt}}/\pi),$$

where $d_{\text{Pt}-\text{Pt}}$ is the average *intra*chain Pt—Pt separation.

At some reduced temperature, referred to as the 3-D ordering temperature T_{3D}, the weak planes of scattering density coalesce into superlattice Bragg spots as a result of the 3-D ordering of the CDWs on *adjacent* metal-atom chains caused by *inter*chain Coulombic interactions. At T_{3D} the waves on adjacent chains have opposite phases (see Fig. 4). Thus η, the *inter*chain coupling parameter, is related to the three-dimensionality of the lattice.

One may differentiate between a dynamic [Kohn anomaly (*21*)] or static lattice distortion [Peierls distortion (PD) (*19*)] using inelastic neutron scattering. As stated previously the Kohn anomaly is a soft

phonon mode at wave vector $2\mathbf{k}_F$ that is the result of a dynamic periodic distortion that arises from electron–phonon interactions. When the temperature is decreased, the energy (frequency) of the $2\mathbf{k}_F$ mode approaches zero (see Fig. 3c), at which point the distortion becomes a static PD.

Because POTCP complexes always contain cations or anions in crystallographic disorder, it is important to point out that the diffuse scattering does not arise from chemical disorder–diffuse scattering. This has been established from the observation that the intensity of the planes of diffuse scattering increases at higher diffraction angles. This rules out disorder–diffuse scattering arising from long-range ordering of anions or cations in the crystal.

Although Comés *et al.* (*78, 93*) were the first to use XDS techniques to measure the $2\mathbf{k}_F$ superstructure lines of KCP(Br), the methods were later taken up by Schultz *et al.* (*70*), Carneiro *et al.* (*62*), and by Braude *et al.* (*94*). Table IV lists the POTCP metals studied that exhibit $2\mathbf{k}_F$ scattering and the DPOs derived from the scattering study compared

TABLE IV

$2\mathbf{k}_F$ VALUES (IN UNITS OF $2\pi/d_{Pt-Pt}$) DETERMINED BY DIFFUSE X-RAY SCATTERING AND CHEMICAL ANALYSIS AND COMPARED TO INTRACHAIN Pt—Pt DISTANCES

Compound	Abbreviation	d_{Pt-Pt} (Å)	$2\mathbf{k}_F$ (chemical)	$2\mathbf{k}_F$ (X-ray)
$K_2[Pt(CN)_4]Br_{0.30} \cdot 3H_2O$	KCP(Br)	2.89	1.70	1.67[a] 1.70[b]
$[C(NH_2)_3]_2[Pt(CN)_4]Br_{0.25} \cdot xH_2O$	GCP(Br)	2.908	1.77	1.75[c]
$K_{1.75}[Pt(CN)_4] \cdot 1.5H_2O$	K(def)TCP	2.965 2.961	1.75	1.76[c] 1.775
$Rb_{1.75}[Pt(CN)_4] \cdot xH_2O$	Rb(def)TCP	2.94	1.75	1.73[c]
$Cs_{1.75}[Pt(CN)_4] \cdot xH_2O$	Cs(def)TCP	2.88	1.75	1.72[c]
$(NH_4)_2(H_3O)_{0.17}[Pt(CN)_4]Cl_{0.42} \cdot 2.83H_2O$	ACP(Cl)	2.92	1.58[d]	1.75[e,f]
$Rb_3(H_3O)_{0.x}[Pt(CN)_4](O_3SO{\cdot}H{\cdot}OSO_3)_{0.49} \cdot (1 - x)H_2O$[g]	RbCP(DSH)	2.826	1.53[h]	1.68[f]
$Cs[Pt(CN)_4](FHF)_{0.39}$	CsCP(FHF)$_{0.4}$	2.833	1.61	1.60[f]

[a] (*78*). [b] (*95*). [c] (*70*).

[d] $2\mathbf{k}_F$ (chemical) was determined from the mole ratios of NH_4^+, Pt, and Cl, before (H_3O^+) was inserted in the formula.

[e] (*62*). [f] (*94*).

[g] The chemical formula given here is the "most likely" formula for RbCP(DSH), based on the crystal structure, probable chemical composition, and X-ray diffuse-scattering measurements (*107*).

[h] This value is for $x = 0$. If $x = 0.12$, then the chemical stoichiometry and the X-ray diffuse scattering are in agreement.

to those obtained from chemical analysis. It should be noted from Table IV that there is generally good agreement between $2\mathbf{k}_F$ as determined by XDS and chemical methods, except for ACP(Cl) and RbCP(DSH). This difference is explained (*62, 96*) by assuming that additional positive charge is present in the crystals as H_3O^+, which counterbalances part of the charge due to the anion, thus rendering inaccurate the determination of the DPO via the $Pt^{2.0+}$ and $Pt^{4.0+}$ ratio deduced from oxidation–reduction titrations. This was eventually understood as resulting from the crystallization of the POTCP complex from a highly acidic solution, which resulted in the incorporation of a hydrated proton species (or more than one species) in the crystal. Finally, the study of diffuse scattering from POTCP compounds has proven to be an invaluable aid in understanding their chemical composition and many related aspects (*1*).

Metal–Metal Bond Lengths and Correlations with DPO

The metal–metal bond lengths in POTCP complexes vary in a systematic manner with the DPO, and Williams (*80*) was the first to point

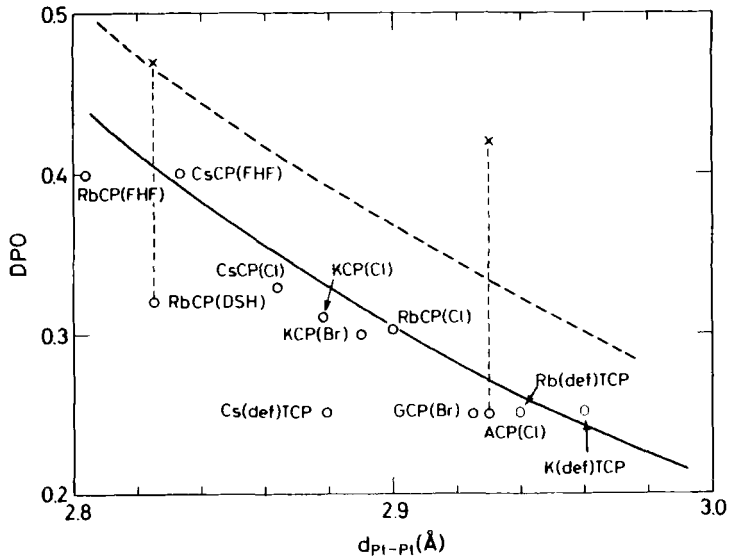

FIG. 14. Plot of the degree of partial oxidation (DPO) versus intrachain Pt—Pt bond lengths for POTCP metals (*80*). Curve (—) is derived using Pauling's formula for metallic resonance, curve (– –) is for no metallic resonance (see *97, 98*). Analysis: x, chemical; O, X-ray diffuse-scattering. The d_{Pt-Pt} spacing for RbCP(Cl) is the average value given in Table III.

out that d_{Pt-Pt} may be calculated from the DPO, and vice versa, using the concept of "metallic resonance" advanced by Pauling (*97*). As originally proposed by Pauling (*98*) $D(n) = D(1) - 0.60 \log_{10} n$, where for a metallic system $D(n)$ is the metallic bond distance for a bond of order n and the single-bond distance is $D(1)$. For POTCP compounds the equation becomes (*80*)

$$d_{Pt-Pt}\,(\text{Å}) = 2.59 - 0.60 \log_{10} \text{DPO},$$

and the derived DPO versus d_{Pt-Pt} values are shown in Fig. 14 for the compounds listed in Table IV. The case of "no metallic resonance" (*98*) is also indicated in Fig. 14. The obvious correlation between DPO and d_{Pt-Pt} suggests that other physical parameters related to these parameters and characterizing POTCP metals may show similar correlations. That this is certainly the case is discussed in the next section.

IV. The Physics of Anion-Deficient POTCP Metals

In Section II we introduced the physics relative to 1-D materials using the tight-binding electron approximation (*99, 100*). However, optical studies of KCP(Br) have shown that the electron-conduction behavior is best described by the free-electron approximation. Nielsen and Carneiro (*101*) have extended the original treatment by Horowitz *et al.* (*102*) of the free-electron case to anion deficient POTCP compounds.

In Table III there are 19 POTCP compounds, and it should be pointed out that the physics of 10 of them has been elucidated in detail in work by Carneiro (*103*) and Underhill *et al.* (*87*).

In order to show continuity in the equations describing the physics of AD POTCP compounds and also to show the interrelation between the structural, chemical, and physical properties of POTCP metals, the reader is reminded that d_{Pt-Pt} and DPO vary regularly and that both quantities are related (*87*) to the Fermi wave vector $\mathbf{k}_F$ namely, the degree of band filling) by

$$\text{DPO} = 2(1 - \mathbf{k}_F d_{Pt-Pt}/\pi). \tag{1}$$

In the intrachain direction the band structure is deduced from free-electron relationships so that the Fermi energy is

$$\varepsilon_F = (h\mathbf{k}_F)^2/4\pi m. \tag{2}$$

Because all of the POTCP compounds exhibit Peierls instabilities, at low temperature a band gap Δ arises where

$$\Delta = 4\frac{1 - \mathbf{k}_F d_{Pt-Pt}/\pi}{1 + \mathbf{k}_F d_{Pt-Pt}/\pi}\varepsilon_F e^{-1/\lambda}, \tag{3}$$

where λ, the dimensionless electron–phonon coupling constant, is given by

$$\lambda = g^2 N(\varepsilon_F)/\omega^0_{2\mathbf{k}_F}, \tag{4}$$

where g is the electrostatic energy gain per relative displacement of the Pt atoms, $N(\varepsilon_F)$ the electronic density of states at ε_F in the metallic phase, and $\omega^0_{2\mathbf{k}_F}$ a bare phonon frequency (*1*). The relationship between the temperature scale T_p of the Peierls instability and Δ is given by

$$T_p = \Delta/(1.77\mathbf{k}_F). \tag{5}$$

Now, from experimental studies using structure analysis, XDS, and dc-conductivity measurements, the values of d_{Pt-Pt}, $\mathbf{k}_F$, and Δ are obtained, and then λ and T_p are computed using Eqs. (3) and (5).

Next, the previously mentioned *inter*chain coupling parameter η, which is defined as the ratio of the bandwidth in the inter- and intrachain directions, allows us to determine the 3-D ordering temperature, which, from the theory of Horowitz *et al.* (*102*) provides

$$T_{3D} = T_p \exp\left(\frac{-2.5}{\eta}\frac{\mathbf{k}_B T_p}{\varepsilon_F}\right). \tag{6}$$

The value of T_{3D}, the 3-D ordering temperature, may be derived (*104*) from the maximum in the logarithmic derivative of the conductivity versus inverse temperature and then, from Eq. (6), η can be determined. For comparison, the *measured* parameters DPO, Δ, and T_{3D} are given in Fig. 15, and the derived *physical* parameters λ and η are shown in Fig. 16.

The most striking features of both Figs. 15 and 16 are the obvious correlations between observed and derived parameters, as shown in the form of rather smooth curves. By inspection it is obvious that the AD compounds are different from the CD derivatives. It is also noteworthy that two types of behavior are obvious from Figs. 15 and 16, that is, (1) there is a steady increase in the electron–phonon coupling λ when d_{Pt-Pt} increases upon going from $Rb_2[Pt(CN)_4](FHF)_{0.4}$ to

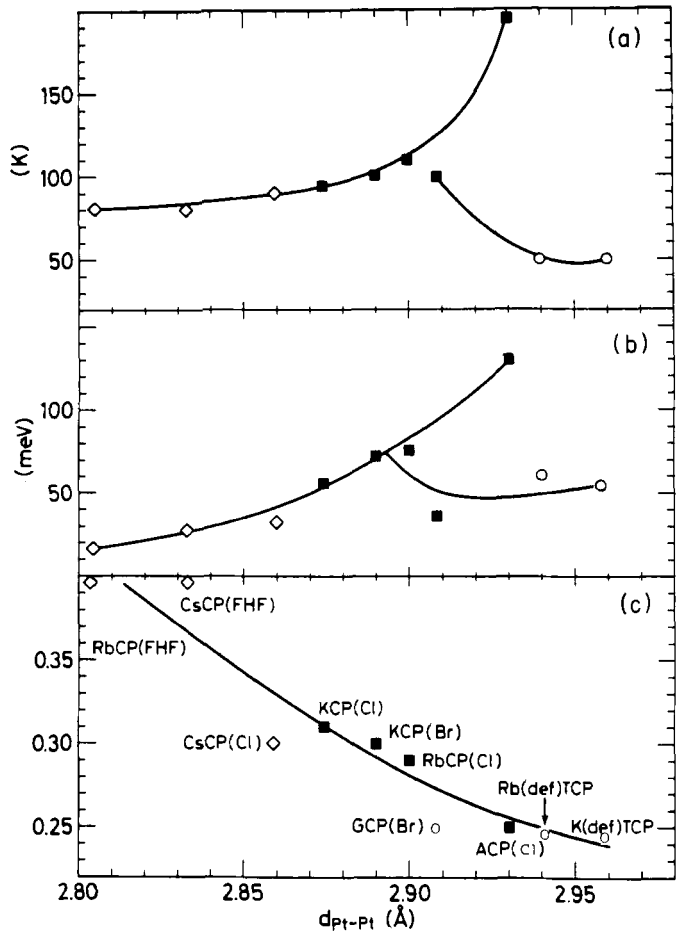

FIG. 15. Plot of the measured values for POTCP metals of the T_{3D} (three-dimensional ordering temperature) (a), △ (band gap) (b), DPO (degree of partial oxidation) (c), and versus d_{Pt-Pt} [intrachain Pt—Pt separation; see (*1*)]. Space groups: ■, *P*4mm; ◇, *I*4/mcm; ○, other.

$NH_4(H_3O)_{0.17}[Pt(CN)_4]Cl_{0.42} \cdot 2.83H_2O$, and (2) there are few exceptions in the regular behavior of AD POTCP compounds, whereas this is not the case for the CD POTCP derivatives, which do not follow the same curves given for the AD metals. Behavior type (1) is explained in terms of the dependence of DPO (and $\mathbf{k}_F$) upon d_{Pt-Pt}, because an increase in $\mathbf{k}_F$ results in a decrease in $\omega^0_{2\mathbf{k}_F}$, which in turn causes an increase in λ [see Eq. (4)]. On the other hand, the DPO versus d_{Pt-Pt} relation appears to "stabilize" ε_F and, therefore, $g^2N(\varepsilon_F)$. It is also noteworthy that in this same series of compounds the interchain coupling η in-

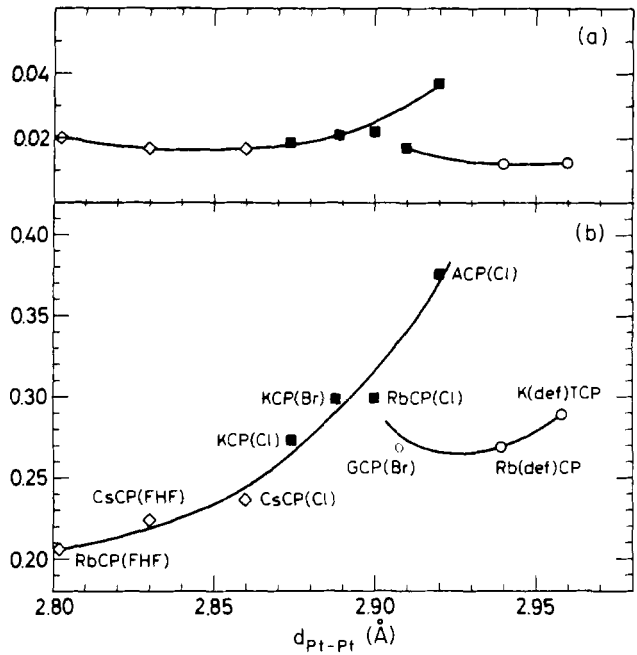

FIG. 16. Plot of the interchain coupling parameter η (a) and electron–phonon coupling constant λ (b), as deduced from experimental studies and plotted versus d_{Pt-Pt}. Space groups: ■, $P4mm$; ◇, $I4/mcm$; ○, other.

creases both for long and short d_{Pt-Pt}s in the presence of increased hydrogen-bonding interactions or more bulky cations. This is a nice demonstration of the effect of "talking between the chains," that is, increased Coulombic interchain coupling and increased electron hopping when the Pt-atom chains come closer together. Behavior type (2) is probably correlated with the more complicated crystal structures and hydrogen-bonding interactions exhibited by the CD salts compared to the AD derivatives.

V. Summary and Conclusions

Clearly, the decade of the 1970s has seen an enormous increase not only in the number of new Pt-chain electrical conductors, but also in the understanding of the chemistry and physics of these materials. A few generalizations are as follows.

1. Partially oxidized tetracyanoplatinate (POTCP) complexes that are hydrated form primitive (type-P) tetragonal lattices (*P4mm*), with the M^+ cations located in one-half of the unit cell and water molecules

in the other half. More importantly, the cations are always located between the planes of the $Pt(CN)_4$ groups. Compounds in this class include KCP(Br), KCP(Cl), RbCP(Cl), (NH_4)CP(Cl), and KCP(FHF).

2. POTCP complexes that are anhydrous form body-centered tetragonal lattices (*I4/mcm*) in which the cations occupy sites in the *same plane* as the $Pt(CN)_4$ groups (type-I). Some of these salts, {e.g., $Rb_2[Pt(CN)_4](FHF)_{0.4}$} have the shortest intra- and interchain Pt—Pt spacings and highest electrical conductivities of all known POTCP salts (*105*). Compounds in this class include CsCP(Cl), $RbCP(FHF)_{0.40}$, $CsCP(FHF)_{0.39}$, and $CsCP(N_3)_{0.25}$ (*106*).

3. Electrical conductivities parallel to the Pt–atom chain, $\sigma_\parallel$, in POTCP metals vary inversely with the *intra*chain Pt—Pt spacing d_{Pt-Pt}. The d_{Pt-Pt} spacings are most dependent on two factors. (1) The degree of partial oxidation (DPO) and d_{Pt-Pt} are inversely related, that is, the Pt-atom chain in a POTCP complex behaves in an accordion-like fashion, depending on the DPO. (2) In a series of isostructural compounds those containing the smaller alkali-metal cations have the shortest d_{Pt-Pt}. For example, RbCP(FHF) < CsCP(FHF) (type-I), and KCP(Br, Cl) < RbCP(Cl) (type-P). In addition, POTCP salts containing smaller cations have a higher tendency to be hydrated which tends to increase d_{Pt-Pt}. POTCP materials have metallic behavior near room temperature, with $\sigma_\parallel$ as high as approximately 2000 Ω^{-1} cm^{-1}, but they become semiconductors at low temperature.

4. POTCP metals have intrachain Pt—Pt spacings of 2.8–2.96 Å, that is, as short as in Pt metal itself (2.775 Å). The d_{Pt-Pt} spacing may be calculated from DPO (*80*).

5. The type-I anhydrous salts, with the shortest d_{Pt-Pt}, have the lowest three-dimensional ordering temperatures (T_{3D}). Therefore, they have the highest electrical conductivities down to the lowest temperatures. These properties are due in part to the absence of hydrogen-bonding interactions.

6. No Na^+ salts and no anhydrous Li^+ POTCP metals have been reported. The synthesis of a POTCP complex with Pt—Pt separations less than in Pt metal might be possible if anhydrous Li^+ or Na^+ derivatives can be prepared.

From the discussion in the text it is quite clear that the POTCP metals have been extensively characterized, and they are well understood because the chemistry and physics of these materials have been worked out hand-in-hand. It appears that new high-conducting Pt-chain metals with even lower semiconductor-transition temperatures than those now known will be developed in the near future.

ACKNOWLEDGMENTS

The author acknowledges the invaluable collaboration of the students and colleagues whose names appear in the cited articles, and he expresses his special thanks to Dr. Arthur J. Schultz, Professor Kim Carneiro, and Professor Allan E. Underhill. Work at Argonne National Laboratory was sponsored by the U. S. Department of Energy, Office of Basic Energy Sciences, Division of Materials Science, under Contract W-31-109-Eng-38. The author also thanks NATO (grants 1276 and 016-81), which made possible collaborative research with foreign scientists.

REFERENCES

1. Williams, J. M., Schultz, A. J., Underhill, A. E., and Carneiro, K., *in* "Extended Linear Chain Compounds" (J. S. Miller, ed.), Vol. I, p. 73. Plenum, New York, 1982. For a comprehensive summary of the known one-dimensional conductors of all types, see Vols. I–III of this treatise.
2. Underhill, A. E., and Watkins, D. M., *Chem. Soc. Rev.* **9,** No. 4, 429 (1980).
3. Williams, J. M., and Schultz, A. J., *NATO Conf. Ser.* [*Ser.*] *6* **1,** 337 (1979).
4. Stucky, G. D., Schultz, A. J., and Williams, J. M., *Annu. Rev. Mater. Sci.* **7,** 301 (1977).
5. Miller, J. S., and Epstein, A. J., *Prog. Inorg. Chem.* **20,** 1 (1976). This article is a comprehensive review of one-dimensional conductors through 1975.
6. Knop, W., and Schneidermann, G., *J. Prakt. Chem.* **37,** 462 (1846).
7. Döbereiner, J. W., *Pogg. Ann.* **28,** 180 (1833).
8. Levy, L. A., *J. Chem. Soc.* p. 1081 (1912).
9. Krogmann, K., *Angew. Chem., Int. Ed. Engl.* **8,** 35 (1969), and references therein.
10. Carneiro, K., ed., "The International Conference of Low-Dimensional Metals," Chemica Scripta Vol. 17, p. 1. Almqvist & Wiksell, Stockholm, 1981.
11. Labes, M. M., Love, P., and Nichols, L. F., *Chem. Rev.* **79,** 1 (1979).
12. Heeger, A. J., and MacDiarmid, A. G., *Chem. Scr.* **17,** 115 (1981).
13. Heeger, A. J., *in* "Highly Conducting One-Dimensional Solids" (J. T. Devreese, R. P. Evrard, and V. E. Van Doren, eds.), p. 69. Plenum, New York, 1979.
14. Bechgaard, K., Jacobsen, C. S., Mortensen, K., Pedersen, H. J., and Thorup, N., *Solid State Commun.* **33,** 1119 (1980).
15. Marks, T. J., and Kalina, D. W., *in* "Extended Linear Chain Compounds" (J. S. Miller, ed.), Vol. 1, p. 197. Plenum, New York, 1982.
16. Reis, A. H., Jr., *in* "Extended Linear Chain Compounds" (J. S. Miller, ed.), Vol. I, p. 157. Plenum, New York, 1982.
17. Whangbo, M.-H., and Hoffmann, R. J., *J. Am. Chem. Soc.* **100,** 6093 (1978).
18. Renker, B., and Comés, R., *in* "Low-Dimensional Cooperative Phenomena" (H. J. Keller, ed.), p. 236. Plenum, New York, 1975.
19. Peierls, R. E., *in* "Quantum Theory of Solids," p. 108. Oxford Univ. Press, London and New York, 1955.
20. Frohlich, H., *Proc. R. Soc. London, Ser. A* **223,** 296 (1954).
21. Kohn, W., *Phys. Rev. Lett.* **2,** 393 (1959).
22. Toombs, G. A., *Phys. Rep.* **40,** 181 (1978).
23. Mott, N. F., *Proc. Phys. Soc., London, Sect. A* **62,** 416 (1949).
24. Hubbard, J., *Proc. R. Soc. London, Ser. A* **281,** 401 (1964).
25. Bardeen, J., Cooper, L. N., and Schrieffer, J. R., *Phys. Rev.* **108,** 1175 (1957).

26. Little, W. A., *Phys. Rev. A* [2] **134,** 1416 (1964).
27. Little, W. A., *J. Polym. Sci., Part C* **29,** 17 (1970).
28. Davis, D., Gutfreund, H., and Little, W. A., *Phys. Rev. B: Solid State* [3] **13,** 4766 (1976). Also see Gutfreund, H., and Little, W. A., *in* "Highly Conducting One-Dimensional Solids" (J. T. Devreese, R. P. Evrard, and V. E. Van Doren, eds.), p. 305. Plenum, New York, 1979.
29. Underhill, A. E., Watkins, D. M., Williams, J. M., and Carneiro, K., *in* "Extended Linear Chain Compounds" (J. S. Miller, ed.), Vol. I, p. 119. Plenum, New York, 1982.
30. Underhill, A. E., *in* "Low-Dimensional Cooperative Phenomena" (H. J. Keller, ed.), p. 287. Plenum, New York, 1975.
31. "Handbook of Chemistry and Physics," 53rd ed., p. F-80. Chem. Rubber Publ. Co., Cleveland, Ohio, 1972–1973.
32. Krogmann, K., and Stephan, D., *Z. Anorg. Chem.* **362,** 290 (1968).
33. Bozorth, R. M., and Pauling, L., *Phys. Rev.* **39,** 537 (1932).
34. Maffly, R. L., Johnson, P. L., and Williams, J. M., *Acta Crystallogr., Sect. B* **33,** 884 (1977).
35. Daniels, W., Yersin, H., Philpsborn, H. V., and Gliemann, G., *Solid State Commun.* **30,** 353 (1979).
36. Moreau-Colin, M. C., *Bull. Soc. R. Sci. Liege* **34,** 778 (1965).
37. Holzapfel, W., Yersin, H., Gliemann, G., and Otto, H. H., *Ber. Bunsenges. Phys. Chem.* **82,** 207 (1978).
38. Johnson, P. L., Musselman, R. L., and Williams, J. M., *Acta Crystallogr., Sect. B* **33,** 3155 (1977).
39. Moreau-Colin, M. C., *Bull. Soc. Miner. Cristallogr.* **91,** 332 (1968).
40. Yersin, H., *J. Chem. Phys.* **68,** 4707 (1978).
41. Koch, T. R., Johnson, P. L., and Williams, J. M., *Inorg. Chem.* **16,** 640 (1977).
42. Washecheck, D. M., Peterson, S. W., Reis, A. H., Jr., and Williams, J. M., *Inorg. Chem.* **15,** 74 (1976).
43. Johnson, P. L., Koch, T. R., and Williams, J. M., *Acta Crystallogr., Sect. B* **33,** 1293 (1977).
44. Otto, H. H., Schultz, H., Thiemann, K. H., Yersin, H., and Gliemann, G., *Z. Naturforsch. B: Anorg. Chem., Org. Chem.* **32B,** 127 (1977).
45. Johnson, P. L., Koch, T. R., and Williams, J. M., *Acta Crystallogr., Sect. B* **33,** 1976 (1977).
46. Williams, J. M., *et al., Inorg. Synth.* **19,** 1–13 (1979).
47. Miller, J. S., *Inorg. Synth.* **19,** 13 (1979).
48. Williams, J. M., *et al., Inorg. Synth.* **20,** 20 (1980).
49. Williams, J. M., *et al., Inorg. Synth.* **21,** 141 (1982).
50. Williams, J. M., work in progress.
51. Williams, J. M., and Schultz, A. J., *Ann. N. Y. Acad. Sci.* **313,** 509 (1978).
52. Toftlund, H., *J. Chem. Soc., Chem. Commum.* p. 837 (1979).
53. Jones, S. A., Taylor, W. H., Holida, M. D., Sutton, L. J., and Williams, J. M., *Inorg. Synth.* **21,** 191 (1982).
54. Williams, J. M., Iwata, M., Peterson, S. W., Leslie, K. A., and Guggenheim, H. J., *Phys. Rev. Lett.* **34,** 1653 (1975).
55. Miller, J. S., and Weagley, R., *Inorg. Chem.* **16,** 2965 (1977).
56. Williams, J. M., Johnson, P. L., Schultz, A. J., and Coffey, C. C., *Inorg. Chem.* **17,** 834 (1978).
57. Brown, R. K., and Williams, J. M., *Inorg. Chem.* **18,** 1922 (1979).

58. Underhill, A. E., Watkins, D. M., and Wood, D. J., *J. Chem. Soc., Chem. Commun.* p. 805, (1976).
59. Brown, R. K., and Williams, J. M., *Inorg. Chem.* **17,** 2607 (1978).
60. Wood, D. J., Underhill, A. E., and Williams, J. M., *Solid State Commun.* **31,** 219 (1979).
61. Johnson, P. L., Schultz, A. J., Underhill, A. E., Watkins, D. M., Wood, D. J., and Williams, J. M., *Inorg. Chem.* **17,** 839 (1978).
62. Carneiro, K., Petersen, A. S., Underhill, A. E., Wood, D. J., Watkins, D. M., and MacKenzie, G. A., *Phys. Rev. B: Condens. Matter* [3] **19,** 6279 (1979).
63. Brown, R. K., Vidusek, D. A., and Williams, J. M., *Inorg. Chem.* **18,** 801 (1979).
64. Underhill, A. E., Coles, G. S. V., Williams, J. M., and Carneiro, K., *Phys. Rev. Lett.* **47,** 1220 (1981).
65. Keefer, K. D., Washecheck, D. M., Enright, N. P., and Williams, J. M., *J. Am. Chem. Soc.* **98,** 233 (1976).
66. Williams, J. M., Keefer, K. D., Washecheck, D. M., and Enright, N. P., *Inorg. Chem.* **15,** 2446 (1976).
67. Reis, A. H., Peterson, S. W., Washecheck, D. M., and Miller, J. S., *J. Am. Chem. Soc.* **98,** 234 (1976).
68. Epstein, A. J., and Miller, J. S., *Solid State Commun.* **29,** 345 (1979).
69. Carneiro, K., Jacobson, C. S., and Williams, J. M., *Solid State Commun.* **31,** 837 (1979).
70. Schultz, A. J., Stucky, G. D., Williams, J. M., Koch, T. R., and Maffly, R. L., *Solid State Commun.* **21,** 197 (1977).
71. Epstein, A. J., and Miller, J. S., *Bull. Am. Phys. Soc.* [2] **22,** 453 (1977); Carneiro, K., and Jacobsen, C., unpublished results.
72. Brown, R. K., Johnson, P. L., Lynch, T. L., and Williams, J. M., *Acta Crystallogr., Sect. B* **34,** 1965 (1978).
73. Schultz, A. J., Coffey, C. C., Lee, G. C., and Williams, J. M., *Inorg. Chem.* **16,** 2129 (1977).
74. Wood, D. J., Underhill, A. E., Schultz, A. J., and Williams, J. M., *Solid State Commun.* **30,** 501 (1979).
75. Schultz, A. J., Gerrity, D. P., and Williams, J. M., *Acta Crystallogr., Sect. B* **34,** 1673 (1978).
76. Although the space group was not determined unambiguously *I4cm* was used. See Stucky, G. D., Putnik, C., Kelber, J., Schaffman, M. J., Salamon, M. B., Pasquali, G., Schultz, A. J., Williams, J. M., Cornish, T. F., Washecheck, D. M., and Johnson, P. L., *Ann. N. Y. Acad. Sci.* **313,** 525 (1978).
77. For reviews and background on X-ray and neutron scattering studies see Comés, R., *in* "One-Dimensional Conductors" (H. G. Schuster, ed.), p. 32. Springer-Verlag, Berlin and New York, 1975; Renker, B., Pintschovious, L., Gläser, W., Rietschel, H., and Comés, R., *ibid.* p. 53; Renker, B., and Comés, R., *in* "Low-Dimensional Cooperative Phenomena" (H. J. Keller, ed.), p. 236. Plenum, New York, 1975.
78. Comés, R., Lambert, M., and Zeller, H. R., *Phys. Status Solidi B* **58,** 587 (1973).
79. Renker, B., Pintschovius, L., Gläser, W., Rietschel, H., Comés, R., Liebert, L., and Drexel, W., *Phys. Rev. Lett.* **32,** 836 (1974).
80. Williams, J. M., *Inorg. Nucl. Chem. Lett.* **12,** 651 (1976).
81. Krogmann, K., and Hausen, H. D., *Z. Anorg. Allg. Chem.* **358,** 67 (1968). A simultaneous study of KCP(Br) was carried out by A. Piccinin and J. Toussaint, *Bull. Soc. R. Sci. Liege* **36,** 122 (1967).

82. Williams, J. M., Petersen, J. L., Gerdes, H. M., and Peterson, S. W., *Phys. Rev. Lett.* **33,** 1079 (1974).
83. See the following articles and references therein: Heger, G., Deiseroth, H. J., and Schultz, H., *Acta Crystallogr., Sect. B* **34,** 725 (1978); Peters, C., and Eagen, C. F., *Inorg. Chem.* **15,** 782 (1976).
84. Miller, J. S., and Epstein, A. J., *Prog. Inorg. Chem.* **20,** 46 (1976).
85. Renker, B., Rietschel, H., Pintschovius, L., Gläser, W., Brüesch, P., Kuse, D., and Rice, M. J., *Phys. Rev. Lett.* **30,** 1144 (1973).
86. Lynn, J. W., Iizumi, M., Shirane, G., Werner, S. A., and Saillant, R. B., *Phys. Rev. B: Condens. Matter* [3] **12,** 1154 (1975).
87. Underhill, A. E., Wood, D. J., and Carneiro, K., *Synth. Met.* **1,** 395 (1979–1980).
88. Carneiro, K., Eckert, J., Shirane, G., and Williams, J. M., *Solid State Commun.* **20,** 333 (1976).
89. Williams, J. M., and Schultz, A. J., *in* "Modulated Structures—1979" (J. M. Cowley, J. B. Cohen, M. B. Salamon, and B. J. Wuensch, eds.), p. 187. Am. Inst. Phys., New York, 1979.
90. Musselman, R., and Williams, J. M., *J. Chem. Soc., Chem. Commun.* p. 186 (1977).
91. Steigmeier, E. F., Baeriswyl, D., Auderset, H., and Williams, J. M., *in* "Quasi One-Dimensional Conductors II" (S. Barisic *et al.*, eds.), p. 229. Springer-Verlag, Berlin and New York, 1979.
92. Williams, J. M., Schultz, A. J., Underhill, A. E., and Carneiro, K., *in* "Extended Linear Chain Compounds" (J. S. Miller, ed.), vol. I, p. 98. Plenum, New York, 1982.
93. Comés, R., Lambert, M., Launois, H., and Zeller, H. R., *Phys. Rev. B: Condens. Matter* [3] **8,** 571 (1973).
94. Braude, A., Lindegaard-Andersen, A., Carneiro, K., and Petersen, A. S., *Solid State Commun.* **33,** 365 (1980).
95. Renker, B., and Comés, R., unpublished results.
96. Williams, J. M., and Schultz, A. J., *NATO Conf. Ser.* [*Ser.*] *6* **1,** 361–363 (1979).
97. Pauling, J., "The Nature of the Chemical Bond and the Structure of Molecules and Crystals," pp. 398–404. Cornell Univ. Press, Ithaca, New York, 1960.
98. Pauling, L., *J. Am. Chem. Soc.* **69,** 542 (1947).
99. Kuse, D., and Zeller, H. R., *Phys. Rev. Lett.* **27,** 1060 (1971); Zeller, H. R., and Brüesch, P., *Phys. Status Solidi* **65,** 537 (1974).
100. Steigmeier, E., Loudon, R., Harbeke, G., Auderset, H., and Scheiber, G., *Solid State Commun.* **17,** 1447 (1975).
101. Nielsen, J. B., and Carneiro, K., *Lect. Notes Phys.* **96,** 238 (1979).
102. Horowitz, B., Gutfreund, H., and Weger, M., *Phys. Rev. B: Solid State* [3] **12,** 3174 (1975).
103. Carneiro, K., unpublished results.
104. Carneiro, K., *NATO Conf. Ser.* [*Ser.*] *6* **1,** 369 (1979).
105. The room temperature electrical conductivity of $RbCP(FHF)_{0.4}$ is $\sim 2000 \Omega^{-1}$ cm^{-1} and is the highest yet reported for a POTCP metal.
106. Both CsCP(Cl) and $CsCP(N_3)_{0.25}$ are not strictly anhydrous but do have type-I molecular structures.
107. Coles, G. S. V., Lindegaard-Andersen, A., Williams, J. M., Schultz, A. J., Brown, R. K., Besinger, R. E., Ferraro, J. R., Underhill, A. E., and Watkins, D. M., *Physica Scripta* **25,** 873 (1982).